JOURNAL OF GEOPHYSICAL RESEARCH, VOL. 102, NO. A12, PAGES 27,137–27,143, DECEMBER 1, 1997

Nonlinear shear Alfvén resonances in a dipolar magnetic field

I. Voronkov, R. Rankin, V. T. Tikhonchuk,[1] and J. C. Samson
Department of Physics, University of Alberta, Edmonton, Alberta, Canada

Abstract. The effect of the ponderomotive force (PF) on the temporal evolution of shear Alfvén field line resonances (FLRs) is considered for a magnetic dipole geometry appropriate to the Earth's magnetosphere. We derive a set of equations which describes the coupling of shear Alfvén and slow mode waves and show that in a dipole field, the PF initiates a spectrum of standing slow mode waves, rather than just the fundamental mode that arises in a Cartesian box model magnetosphere. Magnetic field aligned slow mode density perturbations lead to a nonlinear temporal phase shift between the compressional driver and shear Alfvén wave. This results in nonlinear saturation of the wave fields of FLRs and may occur well in advance of linear saturation as a result of ionospheric dissipation. We derive expressions for the nonlinear frequency shifts caused by the slow mode spectrum and determine the timescale for nonlinear saturation of the shear Alfvén wave fields. Finally, we compare our results with previous estimates made in a box model magnetosphere and show that our main conclusions remain valid.

1. Introduction

Field line resonances (FLRs) are standing shear Alfvén waves (SAWs) that are excited by global compressional Alfvén waves on closed magnetic surfaces in the Earth's magnetosphere. A particular class of ULF oscillations in the corresponding frequency range of Pc5 pulsations is often observed by satellites and ground-based stations [*Walker and Greenwald,* 1981; *Tian et al.,* 1991; *Fenrich et al.,* 1995; *Potemra and Blomberg,* 1996].

According to an idea by *Samson et al.* [1992], FLRs play an important role in auroral dynamics. It is anticipated that FLRs can accumulate energy in localized regions of the magnetosphere and then release it in a short time period of perhaps a few minutes. The overall scenario of the energy transfer in the Earth's magnetosphere is as follows: perturbations in solar wind pressure and magnetic field excite global quasi-monochromatic oscillations corresponding to compressional Alfvén wave (CAW) eigenmodes trapped in the magnetospheric cavity. Because of very rare particle collisions, these waves may persist for long time periods so that the main mechanism for their dissipation will involve their resonant transformation into a SAW. The excited SAWs or FLRs are localized near particular magnetic L shells at which there will appear a spatial concentration of the CAW energy. Providing ionospheric conductivities are high enough, the FLR will narrow and grow to amplitudes where nonlinear effects might limit further growth [*Rankin et al.,* 1993b].

A nonlinear FLR saturation model has been proposed recently by *Rankin et al.* [1994, 1995]. In this model, the ponderomotive force of standing SAWs results in a redistribution of the plasma density along geomagnetic field lines [*Allan et al.,* 1991; *Allan,* 1992, 1993a, b; *Rankin et al.,* 1994, 1995; *Guglielmi,* 1997]. This plasma density redistribution changes the SAW eigenfrequency, detunes the resonance, and periodically decouples the SAW from the CAW driver. The density perturbations along the magnetic field line can be considered as radially localized slow magnetosonic waves (SMWs) that are driven by the ponderomotive force, and therefore the FLR saturation is a result of the nonlinear coupling between SAWs, CAWs, and SMWs. As demonstrated by *Rankin et al.* [1995], the SAW nonlinear frequency shift also results in latitudinal motion and narrowing of the FLR.

The nonlinear FLR model was originally developed using the geometry of straight magnetic field lines (box model) [*Rankin et al.,* 1994, 1995]. Although the qualitative predictions of the model are in agreement with some radar and satellite data (e.g., location of the density depletion, timescale of evolution, and the latitudinal FLR drift [*Rankin et al.,* 1995]), quantitative comparisons cannot be made within the box model because of its neglect of plasma parallel inhomogeneity (and hence the plasma β) and magnetic field line curvature, both of which might be expected to produce significant modifications to the FLR dynamics [*Allan,* 1993a].

This paper presents simplified theory and numerical simulation results for the nonlinear evolution of FLRs

[1] On leave from the P. N. Lebedev Physics Institute, Russian Academy of Science, Moscow.

Paper number 97JA02533.
0148-0227/97/97JA-02533$09.00

in dipolar coordinates. Our model describes the nonlinear coupling between driven SAW and SMW modes and accounts for several features that are not included in the previous box model: (1) We define the region of the most efficient coupling between the CAW and SAW and derive an analytical expression for the FLR amplitude which depends on the driver strength and shift between the driver oscillation frequency and SAW eigenfrequency. (2) In the box model, the spatial structure of SAW and SMW modes is identical. Therefore the SAW couples only to the second spatial SMW harmonic. Conversely, in the dipolar model, the ponderomotive force drives a wide spectrum of SMW eigenmodes which change the dynamics of the FLR saturation. (3) The dipolar model predicts such measurable quantities as spatial FLR structure, the period of pulsations, and the location and magnitude of the density perturbations. These results can be proposed as a guideline for experimental data analysis.

An outline of this paper is as follows. Section 2 describes the main features of the model and the analytical solution for the nonlinear FLR. Section 3 presents numerical results obtained from the solution of the complete set of nonlinear MHD equations. We compare these results with the predictions of the analytical theory. Finally, in section 4 we present our discussion and conclusions.

2. Nonlinear Model of FLRs in Dipolar Geometry

We consider the magnetohydrodynamic (MHD) set of equations:

$$\frac{\partial \mathbf{B}}{\partial t} - \nabla\times(\mathbf{V}\times\mathbf{B}) = 0, \quad (1)$$

$$\rho\frac{\partial \mathbf{V}}{\partial t} + \rho(\mathbf{V}\cdot\nabla)\mathbf{V} + \nabla P - \frac{1}{4\pi}(\nabla\times\mathbf{B})\times\mathbf{B} = 0, \quad (2)$$

$$\frac{\partial p}{\partial t} + \nabla\cdot(\rho\mathbf{V}) = 0, \quad (3)$$

$$\frac{d}{dt}\left(\frac{P}{\rho^\gamma}\right) = 0. \quad (4)$$

In these equations, $\mathbf{B}$ is the magnetic field, $\mathbf{V}$ is the fluid velocity, ρ is the plasma density, P is the thermodynamic pressure, and γ is the adiabatic constant.

We adopt dipolar coordinates (μ, ν, ϕ), where $\mu = \cos\theta/r^2$ is the variable along the magnetic field line, $\nu = \sin^2\theta/r$ numerates magnetic shells, and ϕ is azimuthal. Here (r, θ, ϕ) are spherical coordinates. The corresponding scale factors describe the transition between spherical and dipolar coordinate systems: $h_\mu = r^3/(1+3\cos^2\theta)^{1/2}$, $h_\nu = r^2/(\sin\theta(1+3\cos^2\theta)^{1/2})$, and $h_\phi = r\sin\theta$.

SAWs are initiated by the resonant mode interaction of a monochromatic CAW with a SAW on dipolar magnetic surfaces where the frequency of the compressional mode is close to the natural frequency of the magnetic shell. In reality, compressional modes are excited by some external source such as the solar wind, but if we assume that the CAW absorption rate is small and neglect changes of the CAW amplitude during the evolution of the FLR, we can model the CAW driver as a localized constant amplitude source that is applied in the vicinity of the resonant magnetic surface. We shall also consider low azimuthal wavenumber modes for which the SAWs are mainly toroidal.

The equation for toroidal SAWs follows from the azimuthal components of the Faraday law and momentum equations above:

$$\frac{\partial h_\phi B_\phi}{\partial t} - \frac{1}{h_\nu{}^2}\frac{\partial}{\partial \mu}(h_\nu V_\phi B_\mu) = 0, \quad (5)$$

$$\frac{\partial V_\phi}{\partial t} = \frac{B_\mu}{4\pi\rho h_\mu h_\phi}\frac{\partial h_\phi B_\phi}{\partial \mu} + \omega V_D \sin(\omega t), \quad (6)$$

where the term $\omega V_D \sin(\omega t)$ models the effect of a CAW driver with frequency ω and velocity amplitude V_D which can be taken as having an arbitrary dependence on μ. We assume that V_D is independent of ν. These equations also involve the dipolar magnetic field $B_\mu(\mu, \nu)$ and the plasma density, $\rho = \rho_0 + \delta\rho$, where $\delta\rho$ is the density perturbation due to the ponderomotive force.

It has been shown by *Rankin et al.* [1994, 1995] that the density perturbation $\delta\rho$ is the main nonlinearity in the SAW equation (6). According to the continuity equation (3), the density perturbation couples to the parallel plasma velocity perturbation V_μ and to the plasma pressure perturbation:

$$\frac{\partial \rho}{\partial t} + \frac{1}{h_\mu h_\nu h_\phi}\frac{\partial}{\partial \mu}(h_\nu h_\phi \rho V_\mu) = 0, \quad (7)$$

$$\left[\frac{\partial}{\partial t} + \frac{V_\mu}{h_\mu}\frac{\partial}{\partial \mu}\right]\frac{P}{\rho^\gamma} = 0, \quad (8)$$

$$\rho\frac{\partial V_\mu}{\partial t} + \frac{1}{h_\mu}\frac{\partial P}{\partial \mu} = \rho\frac{V_\phi^2}{h_\mu h_\phi}\frac{\partial h_\phi}{\partial \mu} - \frac{B_\phi}{4\pi h_\mu h_\phi}\frac{\partial h_\phi B_\phi}{\partial \mu} \equiv F_{pm}. \quad (9)$$

The set (5)-(9) describes the coupling between the excited SAW and SMW modes as a result of the ponderomotive force F_{pm}. As compared to the box model, the ponderomotive force in the dipolar geometry has an additional term which is dependant on the magnetic field line curvature.

Note that (5)-(9) neglect the effect of SAW dispersion in the radial direction which is valid only for small azimuthal numbers m and relatively smooth amplitude variation in the radial direction. We return to the discussion of the applicability limits of the model in section 4.

2.1. Linear SAW Eigenmodes

Combining (5) with the homogeneous linear part of (6), one arrives at the linear SAW eigenmode equation

$$\frac{\partial^2 h_\phi B_\phi}{\partial t^2} - \frac{1}{h_\nu^2}\frac{\partial}{\partial \mu}\frac{V_{A0}^2}{h_\phi^2}\frac{\partial}{\partial \mu} h_\phi B_\phi = 0, \qquad (10)$$

where $V_{A0}^2 = B_\mu^2/4\pi\rho_0$ is the square of the Alfvén velocity at the initial moment of time and μ varies from the lower, μ_-, to the upper, μ_+, end of the magnetic field line.

Equation (10) has a fundamental set of eigenmodes $\sim e^{-i\omega_N t} S_N(\mu)$, where ω_N and $S_N(\mu)$ are the mode's eigenfrequency and eigenfunction, respectively. The set of eigenfunctions is orthonormalized as $\int_{\mu_-}^{\mu_+} d\mu h_\nu^2 S_M S_N = \delta_{M,N}$, where $\delta_{M,N}$ is the Kronecker delta function.

Assuming that the driver amplitude is small and that its frequency is close to the SAW eigenmode, $\Delta\omega = \omega_N - \omega \ll \omega$, means that we can introduce the envelope approximation for the SAW: $h_\phi B_\phi = \mathrm{Re}[b_N e^{-i\omega t} S_N(\mu)]$. The equation for b_N follows from (5) and (6) in the linear approximation ($\rho = \rho_0$):

$$\frac{\partial^2}{\partial t^2} h_\phi B_\phi - \frac{1}{h_\nu^2} \times$$

$$\frac{\partial}{\partial \mu}\left[\frac{V_{A0}^2}{h_\phi^2}\frac{\partial}{\partial \mu} h_\phi B_\phi + h_\nu B_\mu \omega V_D \mathrm{Re} i e^{-i\omega t}\right] = 0. \qquad (11)$$

Multiplying this equation by $h_\nu^2 S_M$ and integrating it along the field line, one finds a linear envelope equation for the SAW mode amplitude:

$$\frac{\partial b_N}{\partial t} = -i\Delta\omega b_N + \frac{\omega}{2} R, \qquad (12)$$

where

$$R = \frac{1}{\omega}\int_{\mu_-}^{\mu_+} d\mu h_\nu B_\mu V_D \frac{dS_N}{d\mu} \qquad (13)$$

is an effective driver amplitude. The solution to (12) describes the linear evolution of the driven SAW,

$$h_\phi B_\phi = \frac{\omega R S_N}{\Delta\omega}\cos(\omega t)\sin(\frac{\Delta\omega}{2} t) \qquad (14)$$

and predicts that the central resonant peak of the FLR grows linearly with time and that the width of the resonance narrows with time.

2.2. Slow Magnetosonic Wave Response

From (9), the growth of the amplitude of the SAW results in a corresponding increase in the magnitude of the ponderomotive force F_{pm}. This causes equatorward motion of plasma along geomagnetic field lines and results in a redistribution of the plasma density and pressure. In magnetospheric plasmas, the SMW frequency is much smaller than CAW and SAW frequencies. Therefore we can neglect variations of F_{pm} within the period of the SAW and consider only the time-averaged (over a SAW period) part of F_{pm} in the equations for parallel plasma motion, (7)-(9):

$$\langle F_{pm}\rangle = \frac{|b_N|^2}{8\pi h_\mu h_\phi^2} \times$$

$$\left[\frac{V_{A0}^2}{\omega_N{}^2 h_\mu^2 h_\phi}\frac{\partial h_\phi}{\partial \mu}\left(\frac{\partial S_N}{\partial \mu}\right)^2 - \frac{1}{2}\frac{\partial S_N^2}{\partial \mu}\right]. \qquad (15)$$

Then, (7)-(9) may be reduced to an equation for the pressure variation $\delta P = P - P_0$:

$$\frac{\partial^2}{\partial t^2}\delta P - \frac{C_{S0}^2}{h_\mu^2}\frac{\partial}{\partial \mu}\left(\frac{\partial}{\partial \mu}\delta P - h_\mu \langle F_{pm}\rangle\right) = 0, \qquad (16)$$

where $C_{S0}^2(\mu) = \gamma P_0/\rho_0$ is the square of the acoustic wave velocity at the initial moment of time.

The case $F_{pm} = 0$ provides an equation for free SMW eigenmodes with eigenfrequencies Ω_m and eigenfunctions U_m which are defined as $C_{S0}^2\delta\rho = \sum_m n_m U_m$. It follows from (16) that SMW eigenfunctions satisfy the orthonormality condition

$$\int_{\mu_-}^{\mu_+} d\mu \frac{h_\mu^2}{C_{S0}^2} U_{m_1} U_{m_2} = \delta_{m_1 m_2}. \qquad (17)$$

Integrating (16) over μ with the weight $U_m h_\mu^2/C_{S0}^2$, one can then find an equation for the amplitude of the SMW:

$$\frac{\partial^2 n_m}{\partial t^2} + \Omega_m^2 n_m = -\int_{\mu_-}^{\mu_+} d\mu U_m \frac{\partial}{\partial \mu} h_\mu \langle F_{pm}\rangle$$

$$= \frac{f_m}{2}|b_N|^2, \qquad (18)$$

where $n_m = \mathrm{Re}[n_{0m} e^{-i\Omega_m t}]$. The driving force in (18) is proportional to the local SAW intensity, and the projection f_m of the ponderomotive force on the mth SMW is

$$f_m = \int_{\mu_-}^{\mu_+} d\mu \frac{1}{4\pi h_\phi^2}\frac{\partial U_m}{\partial \mu}\frac{\partial S_N}{\partial \mu} \times$$

$$\left[\frac{V_{A0}^2}{\omega_N{}^2 h_\mu^2 h_\phi}\frac{\partial h_\phi}{\partial \mu}\frac{\partial S_N}{\partial \mu} - S_N\right]. \qquad (19)$$

The solution to (12) provides the following prescription for the amplitude of the driven SMW density perturbations:

$$n_m = \frac{f_m \omega^2 R^2}{4\Omega_m^2 \Delta\omega^2} \times$$

$$\left[\frac{1}{\Omega_m^2 - \Delta\omega^2}(\Delta\omega^2 \cos\Omega_m t - \Omega_m^2 \cos\Delta\omega t) + 1\right]. \qquad (20)$$

The fact that the FLR SAW can excite many SMW harmonics is the result of differences between the mode structure of SAW and SMW eigenfunctions due to the field-aligned spatial inhomogeneity of the system. In the model of homogeneous plasma [*Rankin et al.*, 1994, 1995], the ponderomotive force can only couple directly

to the fundamental mode SMW harmonic, and this coupling ultimately defines the nonlinear dynamics of the FLR.

In order to make the interaction between SAWs and SMWs self-consistent, it is necessary to account for the effect of the SMW density perturbations on the evolution of the driven SAW. It was mentioned above that according to *Rankin et al.* [1994, 1995], the most important nonlinear process affecting the SAW arises from the density perturbations in (6), which can be written as

$$\frac{\partial V_\phi}{\partial t} = \frac{B_\mu}{4\pi\rho_0 h_\mu h_\phi}\left(1-\frac{\delta\rho}{\rho_0}\right)\frac{\partial h_\phi B_\phi}{\partial \mu} + \omega V_D \sin(\omega t). \quad (21)$$

Here we have assumed that the density perturbation is small, $\delta\rho \ll \rho$.

Substituting into (21) the eigenmode expansion of the density perturbations $C_{S0}^2\delta\rho = \sum_m n_m U_m$, where n_m can be found from (18), and repeating the derivation of the envelope equation for the SAW amplitude, one finds that the density perturbation contributes an additional term to (12):

$$\frac{\partial b_N}{\partial t} = i(\Delta\omega_{nl} - \Delta\omega)b_N + \frac{\omega}{2}R, \quad (22)$$

where the nonlinear shift of the frequency of the SAW is defined by

$$\Delta\omega_{nl} = \sum_m n_m \int_{\mu_-}^{\mu_+} d\mu \frac{V_{A0}^2 U_m}{2\omega h_\phi^2 \rho_0 C_{S0}^2}\left(\frac{\partial S_N}{\partial \mu}\right)^2. \quad (23)$$

Equations (18) and (22) describe the nonlinear evolution of externally driven and coupled SAW and SMW modes. In the particular case where only one SMW mode is excited, (18) and (22) coincide exactly with the rectangular box model derived by *Rankin et al.* [1994, 1995]. The difference here is that field-aligned plasma inhomogeneity and magnetic field curvature result in multimode SMW excitation and a more complicated dynamics for the nonlinear evolution of the FLR. However, the general analysis of equations developed by *Rankin et al.* [1994] also holds for the dipolar model.

3. Numerical Solution and Analysis

In this section, we consider the nonlinear evolution of SAWs initiated by an external driver using one-dimensional full MHD simulations and the analytical model described above. We consider an example where the driver frequency resonates with the local SAW at L shell 10. The background density distribution is chosen in the form $\rho_0 = \rho_{eq}(1-\cos\theta^2)^{-q}$, with $\rho_{eq} = 1.044 \times 10^{-24}$ g/cm^3 and $q = 4$. For these parameters, the period T_1 of the first fundamental SAW mode equals 254 s. The plasma pressure is uniform along the field lines in equilibrium. We consider cases corresponding to different plasma temperatures in the equatorial region of the magnetosphere. The CAW driver is modeled by a Gaussian distribution of the velocity along the geomagnetic field line: $V_D(\mu) = V_0 \exp(-l^2/\delta^2)$ with $V_0 = 1.6$ km/s and $\delta = 2\ R_E$. Here l is the distance along the magnetic field line from the equatorial plane.

The temporal evolution of the SAW amplitude b_1, as predicted by (22) and obtained numerically using the complete set of MHD equations, is shown in Figure 1. Time is normalized by the driver period $T = 2\pi/\omega$. In this example, the driver frequency ω is set equal to the eigenfrequency of the SAW fundamental mode. The ambient plasma pressure P_0 is 10^{-10} dyn/cm^2, which corresponds to $\beta = 8\pi P_0/B_\mu^2 = 2.65 \times 10^{-2}$ in the equatorial plane and $\beta = 7.2 \times 10^{-9}$ near to the ionosphere. From Figure 1, it can be seen that the analytical model gives a good prediction of the SAW amplitude evolution during both the linear and nonlinear stages. Similar tests were done for different values of β. The analytical and numerical results are in close agreement.

Now let us consider the influence of the temperature of the plasma in the equatorial plane on the growth and nonlinear saturation of the SAW. Figure 2 shows the time evolution of the SAW amplitude and phase for different equatorial values of β: 2.65×10^{-4}, 2.65×10^{-3}, 2.65×10^{-2}, and 0.88, respectively. It can be seen that nonlinear saturation due to the ponderomotive phase shift of the SAW occurs in all cases, but as expected, lower plasma temperatures lead to faster saturation, so that one could expect to observe higher-amplitude SAWs on field lines which project into hot plasma regions of the equatorial magnetosphere. In fact, very large amplitude FLRs which produce active auroral arcs are seen in the evening sector on field lines threading the high-β region of the plasma sheet [*Samson et al.*, 1996]. In our simulations for the hot plasma case with the driver defined above, the amplitude of the SAW velocity reaches a value of 80 km/s in the equatorial plane. Comparing Figure 2a with Figure 2b, note that in all cases, amplitude saturation coincides with a nonlinear temporal phase shift of $\pi/2$. This is consistent with the results of *Rankin et al.* [1995].

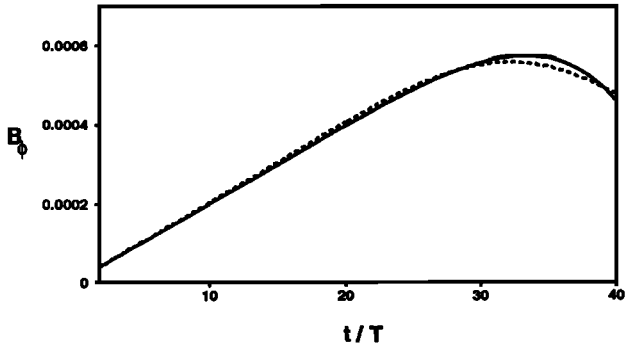

Figure 1. The growth of the amplitude of the shear Alfvén wave (SAW) as predicted by the analytical model (solid line) and obtained numerically from the full set of MHD equations (dashed line). The value β is 2.65×10^{-2} in the equatorial plane; $T = 2\pi/\omega$.

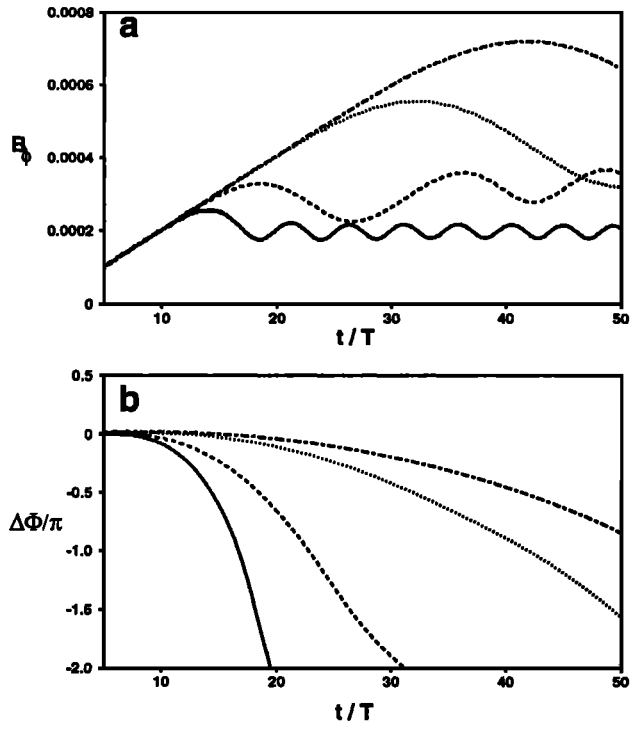

Figure 2. The evolution of the SAW (a) amplitude and (b) phase for $\beta = 2.65 \times 10^{-4}$ (solid line), 2.65×10^{-3} (dashed line), 2.65×10^{-2} (dotted line), and 0.88 (dashed-dotted line). $T = 2\pi/\omega$.

An important feature of the theory of nonlinear dipole FLRs is the coupling of the excited SAW with a spectrum of SMW modes. The temporal evolution of the amplitudes in the SMW spectrum are shown in Figure 3 for the case $\beta = 2.65 \times 10^{-2}$. Amplitudes have been normalized by the maximum amplitude in the SMW spectrum at the moment of time for which each spectrum is computed. One can see that during the initial stage, a wide spectrum of SMW modes is excited. Later, the spectrum becomes sharply peaked at the second spatial harmonic, which is eventually responsible for the nonlinear SAW saturation. Note that it is the second harmonic SMW that has been accounted for in the box model of *Rankin et al.* [1994] which implies that the box model also reasonably predicts the FLR saturation although it falls short in describing the FLR dynamics.

Figure 4 shows the field-aligned distribution of the pressure perturbation at the moment of FLR saturation ($t = 30T$), where T is the driver period. At this time, the SMW perturbation mainly corresponds to the second harmonic with an amplitude $\delta P/P_0 \sim 0.4$ in the equatorial plane. Higher SMW harmonics have smaller amplitudes of the order of a few percent of the ambient pressure. However, it is interesting to note that because of the field-aligned dispersion, these waves are concentrated at distances of $\sim 1 - 2\ R_e$ from the ionosphere, and therefore they might have a significant impact on particle heating and acceleration. Higher-frequency SMW harmonics interact intensively with ions with the rate $\mathrm{Im}\Omega/\mathrm{Re}\Omega \sim 1.1\xi^{7/4}\exp(-\xi^2)$, where $\xi = T_e/T_i$ is the ratio of electron and ion temperatures [*Chen*, 1984].

Another result that is of interest within this model is the growth and saturation of SAWs in the case when the driver frequency is detuned with respect to the SAW eigenfrequency. The amplitude of the SAW is presented in Figure 5 as a function of the frequency shift between the SAW and driver for the case $\beta = 2.65 \times 10^{-2}$ and for different moments of time. Notice that the SAW frequency depends on latitude, and therefore Figure 5 can be considered as the latitude dependance of the FLR amplitude. Initially, the FLR spreads over a wide range of latitudes. Later, the amplitude is peaked around the eigenfrequency of the resonant magnetic shell, and its maximum shifts toward lower-frequency shells.

4. Discussion

The theory of FLRs presented above is an advance from the previous box model [*Rankin et al.*, 1994, 1995] toward a more realistic description of nonlinear FLRs. We have taken into account the dipolar geometry of resonant magnetic shells and the nonuniform distribution of plasma density along geomagnetic field lines. The analytical theory and numerical simulations confirm the main results obtained using the box model. It is shown that the SAW grows because of a resonant coupling with a CAW. In turn, the SAW initiates a ponderomotive force which leads to plasma density redistribution and nonlinear saturation of the FLR due to frequency detuning of the resonant magnetic shell. Compared to the box model, this ponderomotive force consists of three parts: magnetic pressure, magnetic curvature, and particle inertia. We have shown that the density redistribution can be described using an equation for driven SMWs. Owing to the geometry and density inhomogeneity, the coupling between a SAW and nonlinear density perturbations results in the excitation of a wide spectrum of SMWs which gradually form a narrow peak in the vicinity of the second harmonic SMW. The second harmonic SMW is responsible for SAW detuning and FLR saturation. However, the smaller SMW modes may still

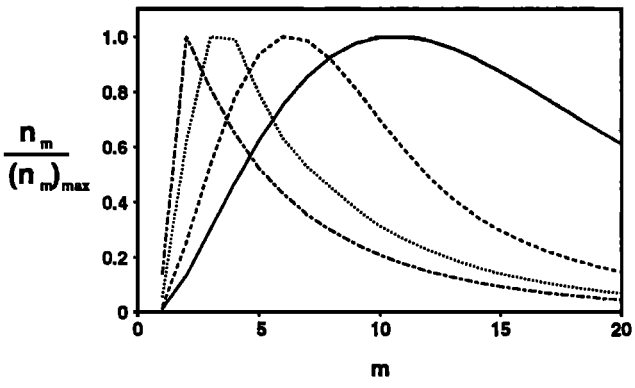

Figure 3. Normalized spectra of acoustic waves, generated by the FLR at time T (solid line), $4T$ (dashed line), $10T$ (dotted line), and $20T$ (dashed-dotted line) for $\beta = 2.65 \times 10^{-2}$ in the equatorial plane; $T = 2\pi/\omega$.

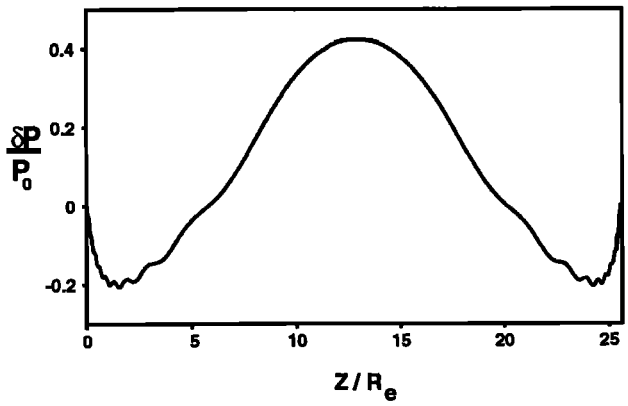

Figure 4. Pressure perturbation distribution along the field line at $t = 30T$. The value $\beta = 2.65 \times 10^{-2}$ in the equatorial plane. The distance Z along the field line is normalized by the Earth's radius R_E, $T = 2\pi/\omega$.

reach significant amplitudes and might play an important role in particle heating at altitudes of 1-2 R_E above the ionosphere. This heating, in conjunction with such mechanisms as two-fluid ponderomotive force acceleration [*Li and Temerin,* 1993], can play an important part in the auroral magnetosphere-ionosphere interaction.

Another result predicted by the dipolar FLR theory is that higher temperatures in the equatorial magnetosphere increase the timescale for ponderomotive FLR saturation, in which case the FLR SAW can grow to large amplitude. This result appears to be in agreement with an observed latitudinal distribution of Pc5 pulsations which have a maximum in the region corresponding to the hot plasmas of the ring current belts [*Walker and Greenwald,* 1981; *Tian et al.,* 1991; *Potemra and Blomberg,* 1996] and of the evening sector of the inner plasma sheet [*Samson et al.,* 1996].

Neglecting plasma wave dispersion across magnetic L shells [*Streltsov and Lotko,* 1996], we have found that the FLR should evolve into a narrow channel near a resonant shell which can eventually lead to Kelvin-Helmholtz shear flow instabilities [*Rankin et al.,* 1993a].

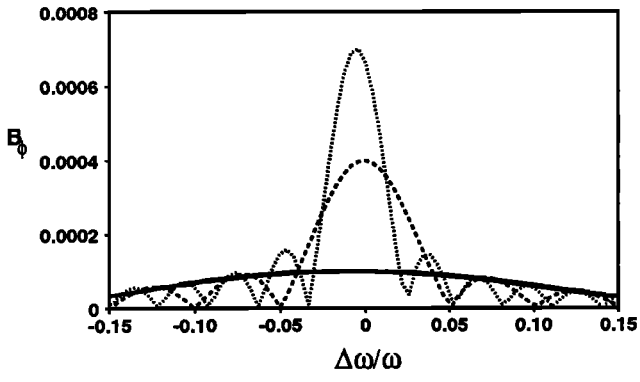

Figure 5. SAW amplitudes as a function of the frequency shift between the driver and SAW at time $5T$ (solid line), $20T$ (dashed line), $35T$ (dotted line). The value $\beta = 2.65 \times 10^{-2}$ in the equatorial plane; $T = 2\pi/\omega$.

However, this result requires the further development of the model to take into account the radial gradients of plasma parameters.

In this study, we assumed that ionospheric conductivities are infinitely high. Low conductivity may cause energy dissipation from the Pedersen currents and the interaction of the toroidal and poloidal modes because of the Hall current [*Allan and Knox,* 1979]. Another dispersive mechanism which can affect the nonlinear evolution of FLRs is azimuthal gradients of high-amplitude SAWs. This effect can be significant for large-m (small azimuthal wavelength) SAWs [*Klimushkin et al.,* 1995]. These waves have been observed in the midnight sector of the magnetosphere, whereas small-m FLRs appear in the dawn and dusk sectors [*Fenrich et al.,* 1995]. The detailed modeling of these effects will be addressed in future investigations.

Acknowledgments. This research was supported by the Natural Sciences and Engineering Research Council of Canada (NSERC), the Canadian Space Agency, and the Russian Foundation for Basic Research under grant 96-02-16707-a.

The Editor thanks M. A. Temerin and A. D. M. Walker for their assistance in evaluating this paper.

References

Allan, W., Ponderomotive mass transport in the magnetosphere, *J. Geophys. Res., 97,* 8483, 1992.

Allan, W., The ponderomotive force of standing Alfvén waves in a dipolar magnetosphere, *J. Geophys. Res., 98,* 1409, 1993a.

Allan, W., Plasma energization by the ponderomotive force of magnetospheric standing Alfvén waves, *J. Geophys. Res., 98,* 11383, 1993b.

Allan, W., and F.B. Knox, A dipole field model for axisymmetric Alfvén waves with finite ionosphere conductivities, *Planet. Space Sci., 27,* 79, 1979.

Allan, W., J. R. Manuel, and E. M. Poulter, Magnetospheric cavity modes: Some nonlinear effects, *J. Geophys. Res., 96,* 11461, 1991.

Chen, F. F., *Introduction to Plasma Physics and Controlled Fusion,* vol. 1, *Plasma Physics,* Plenum, New York, 1984.

Fenrich, F. R., J. C. Samson, J. Sofko, and R. A. Greenwald, ULF high- and low-m field line resonances observed with the Super Dual Auroral Radar Network, *J. Geophys. Res., 100,* 21535, 1995.

Guglielmi, A. V., Comment on the ponderomotive self-action of Alfvén waves, *J. Geophys. Res., 102,* 209, 1997.

Klimushkin, D. Y., A. S. Leonovich, and V. A. Mazur, On the propagation of transversally small-scale standing Alfvén waves in a three-dimensionally inhomogeneous magnetosphere, *J. Geophys. Res., 100,* 9527, 1995.

Li, X., and M. Temerin, Ponderomotive effects on ion acceleration in the auroral zone, *Geophys. Res. Lett., 20,* 13, 1993.

Potemra, T. A., and L. G. Blomberg, A survey of Pc5 pulsations in the dayside high-latitude regions observed by Viking, *J. Geophys. Res., 101,* 24801, 1996.

Rankin, R., B. G. Harrold, J. C. Samson, and P. Frycz, The nonlinear evolution of field line resonances in the Earth's magnetosphere, *J. Geophys. Res., 98,* 5839, 1993a.

Rankin, R., J. C. Samson, and P. Frycz, Simulations of driven field line resonances in the Earth's magnetosphere, *J. Geophys. Res., 98,* 21341, 1993b.

Rankin, R., P. Frycz, V. T. Tikhonchuk, and J. C. Samson, Nonlinear standing shear Alfvén waves in the Earth's magnetosphere, *J. Geophys. Res., 99,* 21291, 1994.

Rankin, R., P. Frycz, V. T. Tikhonchuk, and J. C. Samson, Ponderomotive saturation of magnetospheric field line resonances, *Geophys. Res. Lett., 22,* 1741, 1995.

Samson, J. C., B. G. Harrold, J. M. Ruohoniemi, R. A. Greenwald, and A. D. M. Walker, Field line resonances associated with MHD waveguides in the magnetosphere, *Geophys. Res. Lett., 19,* 441, 1992.

Samson, J. C., L. L. Cogger, and Q. Pao, Observations of field line resonances, auroral arcs, and auroral vortex structures, *J. Geophys. Res., 101,* 17373, 1996.

Streltsov, A., and W. Lotko, The fine structure of dispersive, nonradiative field line resonance layers, *J. Geophys. Res., 101,* 5343, 1996.

Tian, M., T. K. Yeoman, M. Lester, and T. B. Jones, Statistics of Pc5 pulsation events observed by SABRE, *Planet. Space Sci., 39,* 1239, 1991.

Walker, A. D. M., and R. A. Greenwald, Statistics of occurrence of hydromagnetic oscillations in the Pc5 range observed by the STARE auroral radar, *Planet. Space Sci., 29,* 293, 1981.

R. Rankin, J. C. Samson, V. T. Tikhonchuk, and I. Voronkov, Department of Physics, University of Alberta, Edmonton, Alberta, Canada, T6G 2J1. (e-mail: igor@space.ualberta.ca, rankin@space.ualberta.ca, samson@space.ualberta.ca)

(Received July 10, 1997; revised September 4, 1997; accepted September 5, 1997.)